Available online at www.sciencedirect.com

ScienceDirect

Energy Procedia 55 (2014) 287 – 294

Energy Procedia

4th International Conference on Silicon Photovoltaics, SiliconPV 2014

Codiffused bifacial n-type solar cells (CoBiN)

Philip Rothhardt[a,*], Sebastian Meier[a], Carsten Demberger[b], Andreas Wolf[a], Daniel Biro[a]

[a]*Fraunhofer Insitute for Solar Energy Systems (ISE), Heidenhofstrasse 2, 79110 Freiburg, Germany*
[b]*Gebr. SCHMID GmbH, Robert-Bosch-Strasse 32-34, 72250 Freudenstadt, Germany*

Abstract

We present codiffused bifacial n-type (CoBiN) solar cells on 156 mm Czochralski grown (Cz) Si wafers with peak efficiencies of 19.6 % fabricated using a lean industrial process. Simultaneous diffusion of phosphorus back surface field (BSF) and boron emitter in one single tube furnace process, the so called codiffusion, leads to a significant process simplification. Manipulation of the borosilicate glass (BSG) layer, deposited by atmospheric pressure chemical vapor deposition (APCVD) prior to the $POCl_3$ based codiffusion process, allows for emitter profile tuning, without influencing the phosphorus doped BSF. Analytical simulations concerning the BSF identify the dark saturation current density of the passivated part of the BSF $J_{0pass,\ BSF}$ as the parameter that allows for maximum improvement of cell efficiency.

Peer-review under responsibility of the scientific committee of the SiliconPV 2014 conference

Keywords: Codiffusion; n-type; bifacial; APCVD

1. Introduction

Many applications in research have demonstrated the high efficiency potential of n-type silicon solar cells[1, 2]. The increase in efficiency compared to p-type Czochralski (Cz) solar cells is mainly due to a reduced bulk recombination. This is caused by a higher tolerance to common metallic impurities and the absence of B-O complexes and thus light induced degradation[3]. One major difference between n and p-type solar cells is that n-type solar cells in general exhibit at least two diffused areas e.g. a boron doped emitter and a phosphorus doped back surface field (BSF). In state of the art processing these areas are diffused in separate high temperature steps using gaseous sources, e.g. BBr_3- and $POCl_3$-atmospheres [4]. The additional diffusion step, compared to p-type solar cell

* Corresponding author. Tel.: +49-761-4588-5059; fax: +49 761 4588-9250.
E-mail address: Philip.rothhardt@ise.fraunhofer.de

Peer-review under responsibility of the scientific committee of the SiliconPV 2014 conference
doi:10.1016/j.egypro.2014.08.084

manufacturing implicates additional process complexity and process cost.

To avoid this additional effort, many different approaches exist to form boron emitter and phosphorus BSF in one single high temperature step, the so called codiffusion. Approaches that have been performed so far include diffusion from screen printing pastes (efficiency: 8.5%) [5], diffusion from solid (plasma enhanced chemical vapor deposition) and gaseous sources (efficiency of 17.2%)[6, 7] and ion implantation (cell efficiency 18.6%) [8].

In this work we present codiffusion from a $POCl_3$ atmosphere and a BSG layer deposited by atmospheric pressure chemical vapor deposition (APCVD). The main advantage of this approach is its industrial feasibility. Diffusion furnaces for $POCl_3$ diffusion already exist in current productions lines for standard p-type solar cells. The only upgrade needed for the diffusion process are APCVD-machines which are known to be suitable for large scale industrial production e.g. from experience in the microchip industry and represent a cost effective deposition method without any need of vacuum technology.

After presenting experimental results concerning the phosphorus diffusion in earlier publications[9], here we investigate boron emitter formation and present cell results from an industrial process as well as simulations concerning the phosphorus doped BSF.

2. Experiment and method

2.1. Experiment: cell fabrication

Bifacial n-type solar cells (Fig.1) are fabricated according to the process sequence presented in Fig. 2. Exclusively industrial type production equipment at the pilot line PV-TEC at Fraunhofer ISE and at SCHMID Group is used for fabrication. We use 156 mm x 156 mm pseudosquare n-type Cz Si wafers with a base resistivity of 3 to 6 Ωcm. After alkaline texturing, a BSG layer covered by a SiO_x capping layer is deposited by APCVD on one side of the wafers in one deposition process using an APCVD inline tool by SCHMID Group. Then wafers are subjected to a $POCl_3$ based codiffusion process[9, 10]. A hydrofluoric acid based (HF) solution then removes the resulting PSG layer as well as the BSG and SiO_x capping layer. Now the boron emitter is passivated by a stack consisting of 4 nm Al_2O_3 covered by 70 nm of SiN_x and the phosphorus BSF by a SiN_yO_z/SiN_x stack[11]. The Al_2O_3 is deposited by atomic layer deposition using an inline tool, the other layers by plasma enhanced chemical vapor deposition (PECVD). An H-Grid is printed on both sides of the wafer using screen printing applying single print on both sides. While the paste on the phosphorus doped BSF is the same paste that is commonly used to contact the emitter of a p-type cell, the paste contacting the boron emitter contains silver and aluminum. After contact formation in a belt furnace a laser edge isolation may be performed. The presented cell efficiency is determined at Fraunhofer ISE Callab PV Cells using two different measurement chucks, before laser edge isolation, while the IV-data in Fig. 3 is measured after laser edge isolation in order to eliminate any influence of the parallel resistance.

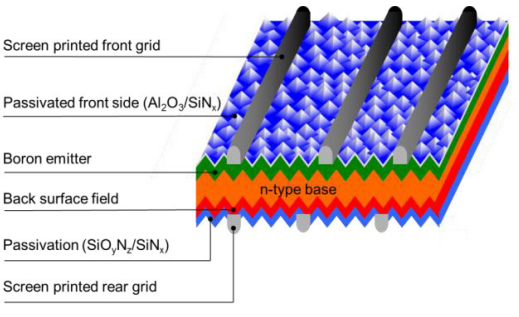

Fig. 1. Schematic view of a bifacial solar cell featuring a boron emitter passivated by a Al_2O_3/SiN_x layer stack and a full area BSF.

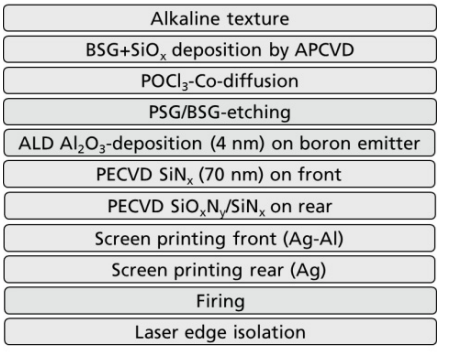

Fig. 2. Process sequence for the fabrication of codiffused bifacial n-type solar cells (CoBiN).

2.2. Simulation

The aim of the simulation is investigating the effect of the full area BSF on efficiency of bifacial n-type solar cells (Fig. 1). In order to explore this context, we conducted simulations using the analytical software Gridmaster [12], which is based on the two diode model. We will first discuss our general approach and then list the input parameters used.

For an exact description of the influence of the BSF on solar cell performance many parameters are needed which significantly complicates interpretation. For the sake of simplicity we selected four parameters with the aim to cover the most important electrical properties of a BSF: Conductivity, represented by the sheet resistance R_{sh}, recombination activity in the passivated and metallized area $J_{0pass,BSF}$ and $J_{0met,BSF}$, and specific contact resistance of the screen printed metallization ρ_c. These four parameters in turn influence all cell parameters, meaning open circuit voltage V_{oc}, fill factor FF and short circuit current density J_{sc}. To allow for an analytical treatment of this problem we neglected the influence of free carrier absorption in the BSF on J_{sc}, this means that we consider the effect of the BSF on V_{oc} and FF. Since to our knowledge no analytical model for spreading resistance in PERT cells is available, we assume lateral current flow in the base and the BSF. This approximation is valid for high pitches. Since in this paper the wafer thickness is smaller than the pitch, we assume this approximation to be valid.

Table 1 depicts the constant input parameters used for simulation.

Table 1. Constant input parameters used for analytical simulations presented in Section 3.2.

Base resistivity [Ωcm]	Base thickness [µm]	Rear finger width [µm]	Rear busbar width [µm]	$J_{0e+base}$ [fA/cm²]	J_{02} [nA/cm²]	J_{sc} [mA/cm²]
1.5	180	60	1500	180	15	39

We assumed a base resistivity of 1.5 Ωcm and a final wafer thickness of 180 µm. For the rear side metallization we used a finger width of 60 µm, continuous busbars with a width of 1500 µm. The cumulated recombination of the passivated and metallized parts of the emitter as well as the base sum up to $J_{0e+base}$ 180 fA/cm² and J_{02} of 15 nA/cm². For passivated area of the BSF we estimate a contribution to J_{02} of $J_{02pass,BSF}$=12 nA/cm². The short circuit current J_{sc} is set to 39 mA/cm². Since we simulate front side illumination only, the rear side grid does not cause any shading losses.

Fig. 4-8 present calculated values for cell efficiency and rear side finger pitch. These values are plotted over the dark saturation current density of the passivated part of the BSF $J_{0pass,BSF}$ and one of the following three parameters: the dark saturation current density of the metalized part of the BSF $J_{0met,BSF}$, the specific contact resistance of screen printed contacts on the BSF ρ_c and the sheet resistance of the BSF R_{sh}. If any of the parameters is constant, we use the values depicted in table 2.

Table 2. input parameters: for each figure, one parameter is varied while the other two are kept constant.

$J_{0met,BSF}$ [fA/cm²]	ρ_c [mΩcm²]	R_{sh} [Ω/sq.]
706	3.6	70.4

For Fig. 4, 6 and 7 the presented efficiency is calculated as follows: For each set of $J_{0pass,BSF}$, $J_{0met,BSF}$, ρ_c and R_{sh} the rear side finger pitch is varied until a maximum efficiency is reached. Please note that the finger pitch is not constant over the plot but adjusted for maximum efficiency if not otherwise stated. The star like symbols in Fig. 4-8 represent experimentally obtained combination of parameters for BSFs resulting from different codiffusion processes [13].

3. Results and discussion

In this chapter we first present the influence of the diluted diborane gas flow during the APCVD deposition process on IV parameters and cell efficiencies. The second part comprises simulation results concerning the phosphorus doped BSF, amongst others the influence of its electrical parameters on cell efficiency.

3.1. Experimental: cell results

One challenge when optimizing codiffusion processes is the independent manipulation of phosphorus and boron doping profiles. Since many parameters that are commonly used to change doping profiles, e.g. temperature and O_2 gas flow, influence both the boron and the phosphorus doping profile, suitable parameters have to be identified that only affect the diffusion of either boron or phosphorus. For the phosphorus diffusion such a parameter is the N_2-$POCl_3$ gas flow[13]. For the boron diffusion we believe that such a parameter is the diluted diborane gas flow during the APCVD deposition process.

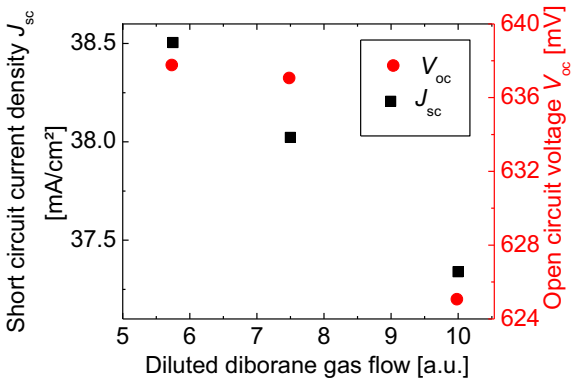

Fig. 3. Influence of diluted diborane gas flow during APCVD deposition on IV-parameters of bifacial n-type solar cells fabricated by codiffusion.

Fig. 3 presents the influence of the diluted diborane gas flow during APCVD deposition on IV parameters of solar cells fabricated according to the process sequence depicted in Fig. 2. It is well known from literature that a decrease in diborane gas flow leads to a decrease in boron concentration in the deposited BSG layer and thus a decrease in emitter doping[14]. This is consistent with the findings in Fig. 3: A decrease in diborane gas flow leads to a decrease in emitter doping concentration, which reduces free carrier absorption and recombination, increasing both J_{sc} and V_{oc}. During the $POCl_3$ based high temperature step the BSG layer is separated from the gaseous atmosphere by a SiO_x capping layer. Thus we assume that a change in the BSG does not influence the phosphorus doping on the cells' rear side, experimental verification is still pending though.

Table 3 presents the peak efficiency for a CoBiN cell processed according to the process flow depicted in Fig. 2 measured before laser edge isolation. Since no international measurement standards for bifacial solar cells exist, two different measurements are performed. The first measurement is performed with a non-reflective chuck that only contacts the solar cells busbars. For the second measurement a reflective and conductive chuck is used that contacts the whole rear side of the solar cell.

Table 3. Cell efficiencies of CoBin solar cells measured at Fraunhofer ISE CalLab

Measurement chuck	V_{oc} [µm]	J_{sc} [mA/cm²]	*FF* [%]	*η* [%]
Non reflective, contacts busbars	643	38.6	77.5	19.3
Reflective , full area contact	645	39.0	78.0	19.6

The peak efficiency of 19.6 % shows the suitability of $POCl_3$-based diffusion processes for the fabrication of high efficiency n-type solar cells. We believe that this efficiency in combination with the short process sequence proves the industrial relevance of this cell concept. While the number of process steps as well as cell efficiency is similar to those of p-type passivated emitter and rear cells, this cell design does not suffer from light induced degradation. Additionally the inherent bifaciality allows for additional energy yield. The parallel resistance before edge isolation is 1.7 kΩcm² and increases to 11.7 kΩcm² after laser edge isolation, wheras cell efficiency is almost unchanged due to the loss in J_{sc} caused by reducing the active cell area.

3.2. Simulation: influence of BSF on cell efficiency

One main aim of this chapter is to connect single electric properties of the BSF (R_{sh}, $J_{0pass,BSF}$, $J_{0met,BSF}$, ρ_c) with cell efficiency. For this purpose, simulations are necessary, because experimentally changing only one of these parameters while leaving the others unchanged is extremely difficult. In order to connect simulation and experiment we also show experimentally obtained data pairs of the respective x and y coordinate[13]. Doing this we hope to give an example how the respective x and y coordinate are linked experimentally. We would further like to suggest some rough approximations that might help when tuning diffusion processes for phosphorus doped BSFs. Simulations are performed using the analytical software Gridmaster[12] and the assumptions described in Section 2.2. Since a common property to characterize a BSF is its sheet resistance, Fig. 4 presents the influence of sheet resistance R_{sh} and dark saturation current density in the passivated area $J_{0pass,BSF}$ on the efficiency of a bifacial n-type solar cell (Fig. 1).

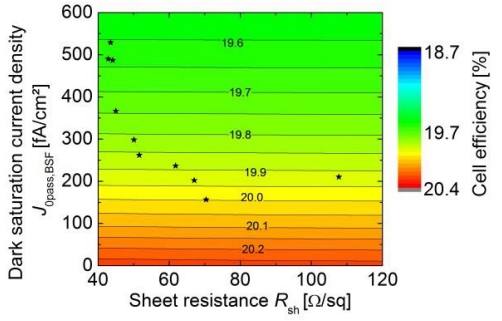

Fig. 4. Cell efficiency over $J_{0pass,BSF}$ and R_{sh} for constant $J_{0met,BSF}$ and ρ_c. The rear side finger pitch is adjusted for maximum efficiency (compare fig 5). Symbols represent experimental data.

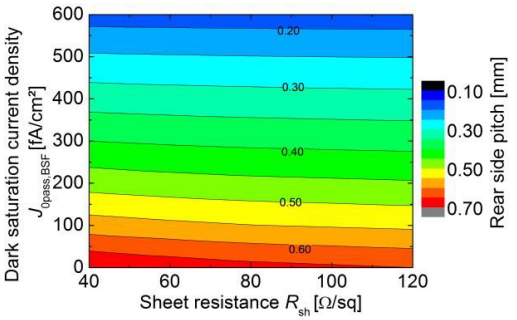

Fig. 5. Optimum rear side finger pitch over $J_{0pass,BSF}$ and R_{sh} for constant $J_{0met,BSF}$ and ρ_c.

Fig. 4 points out that while a change in $J_{0pass,BSF}$ has a large influence on cell efficiency the influence of sheet resistance on cell efficiency is comparatively small. In order to understand the small influence of R_{sh} on efficiency Fig. 5 shows the corresponding finger pitch of the screen printed metallization on the BSF. For an increase in R_{sh} the pitch decreases and thus compensates the loss in conductivity. Thus as long as silver consumption is not an issue, no

light is incident on the cells' rear side and base resistivity is sufficiently low (in this case 1.5 Ωcm), the diffusion process should be optimized for minimum $J_{0pass,BSF}$ without considering the change in sheet resistance.

One way to decrease $J_{0pass,BSF}$ is to decrease BSF doping thus reducing surface and Auger recombination. Unfortunately this decreases surface shielding and increases the dark saturation current density $J_{0met,BSF}$ of the metalized area. To quantify the trade-off between decreased recombination in passivated areas and increased recombination under the metal contacts Fig. 6 presents the influence of $J_{0pass,BSF}$ and $J_{0met,BSF}$ on cell efficiency.

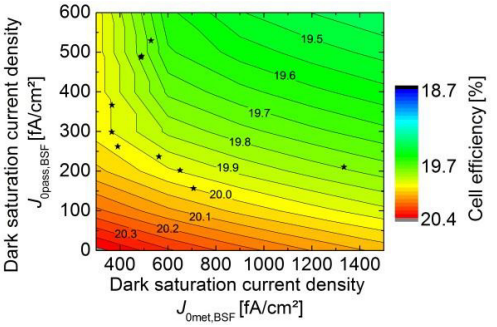

Fig. 6. Cell efficiency over $J_{0pass,BSF}$ and $J_{0met,BSF}$ for constant R_{sh} and ρ_c. Symbols represent experimental data.

For the theoretical case of $J_{0pass,BSF} > J_{0met,BSF}$ (upper left corner of Fig. 6) the efficiency is only dependent on $J_{0met,BSF}$, since the whole rear side is metalized. Beyond this area both a decrease in $J_{0pass,BSF}$ and $J_{0met,BSF}$ increase efficiency. In this case the lines of constant efficiency allow to quantify when a change in the dark saturation current density in the passivated area ($\Delta J_{0pass,BSF}$) is compensated by an increase in the dark saturation current density in the metalized area ($\Delta J_{0met,BSF}$). More concrete: for $6 \times \Delta J_{0pass,BSF} \approx -\Delta J_{0met,BSF}$ cell efficiency stays constant. When taking a look at the experimental values in Fig 6, it seems that in general $6 \times \Delta J_{0pass,BSF} << -\Delta J_{0met,BSF}$ holds. Thus the influence of $J_{0pass,BSF}$ dominates over the influence of $J_{0met,BSF}$ and a decrease in $J_{0pass,BSF}$ leads to an increase in cell efficiency. So again $J_{0pass,BSF}$ is the parameter of choice for increasing efficiency.

The next paragraph discusses the trade-off between recombination and specific contact resistance. Qualitatively this trade-off is simple. A decrease in (surface) doping concentration generally decreases recombination and increases contact resistance, which increases V_{oc} and decreases FF. A quantitative understanding of this relation is more complex though.

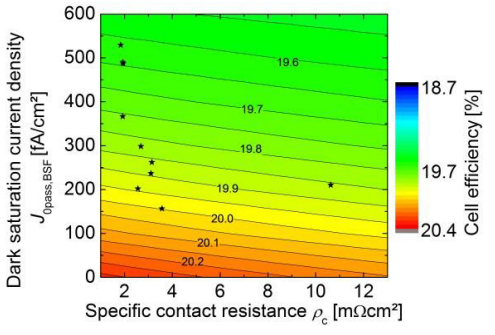

Fig. 7. Cell efficiency over $J_{0pass,BSF}$ and ρ_c for constant R_{sh} and $J_{0met,BSF}$. Please note that the rear side finger pitch is different for each combination of $J_{0pass,BSF}$ and ρ_c. Symbols represent experimental data.

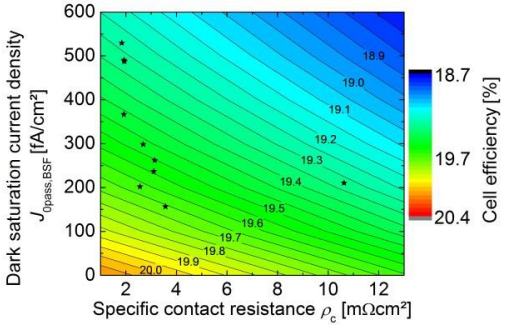

Fig. 8. Cell efficiency over $J_{0pass,BSF}$ and ρ_c for constant R_{sh}, $J_{0met,BSF}$ and a constant pitch of 1.9 mm. Symbols represent experimental data.

Fig 7 presents cell efficiency over $J_{0pass,BSF}$ and ρ_c. As expected a decrease in both $J_{0pass,BSF}$ and ρ_c increases cell efficiency. Quantitatively the lines of constant efficiency are characterized by $\Delta J_{0pass,BSF}/(fA/cm^2) \approx -6.5\ \Delta\rho_c/(m\Omega cm^2)$. Please note that this relation only holds if the rear side finger pitch is adapted for maximum efficiency. More specific the finger pitch applied in Fig. 7 varies between 0.1 and 0.8 mm, which is not an option in industrial production. If cost is important, the finger pitch cannot be varied at will, but needs to be as high as possible to decrease silver consumption. In order to factor this in, Fig. 8 shows cell efficiency calculated from the same input parameters as used in Fig. 7. The difference is that the finger pitch in Fig. 8 is set at a constant value of 1.9 mm, which is comparable to front side metallization of p-type solar cells. When comparing Fig. 7 and 8 it becomes clear that for low $J_{0pass,BSF}$ and ρ_c the difference in efficiency is ~ 0.2 % absolute while for high $J_{0pass,BSF}$ and ρ_c the difference in efficiency of ~ 0.8 % absolute is larger. This means that for high efficiencies the optimum rear side finger pitch of bifacial solar cells approaches the front side finger pitch of a p-type solar cell. A second finding, this figure may also serve for comparing cell efficiencies. As a very rough rule of thumb one may assume a maximum loss in efficiency of 0.2-0.3 % absolute for solar cells with efficiencies around 20 % when changing from a rear side grid that is optimized for maximum cell efficiency to a rear side grid that is similar to the front side grid of a p-type cell. A third interesting fact is that the slope of the lines for constant efficiency in Fig. 8 is different from those in Fig. 7. For high efficiencies the lines of constant efficiency in Fig. 8 may be described by $\Delta J_{0pass,BSF}/(fA/cm^2) \approx -18\ \Delta\rho_c/(m\Omega cm^2)$. Thus for a fixed finger pitch of 1.9 mm the slope changes roughly by a factor of 3 compared to Fig. 7 with a variable pitch. When looking at the experimental data it follows again that a reduction in $J_{0pass,BSF}$ in general leads to an increase in cell efficiency. The only exception been the data point at $J_{0pass,BSF} \approx 200\ fA/cm^2$ and $\rho_c \approx 11\ m\Omega cm^2$. Combining the findings from all figures we follow that a promising approach to BSF optimization is to focus on the reduction of $J_{0pass,BSF}$. We hope that the quantitative approximations presented in this paragraph allow for a more directed development of diffusion processes for bifacial n-type solar cells.

4. Conclusion

In this work we study experimentally codiffusion processes from APCVD deposited borosilicate glass and an atmosphere containing $POCl_3$. We present large area solar cells with peak efficiencies of 19.6 % produced using a lean industrial process and only industrial type equipment. We show that boron emitter manipulation is possible by tuning the diborane gas flow during the APCVD deposition process. Simulations predict that for maximum efficiency minimizing the dark saturation current density in the passivated area of the BSF promises the largest increase in cell efficiency.

Acknowledgements

The authors would like to thank the PV-TEC team for processing and SCHMID for support concerning the APCVD processes. This work was funded by the German Federal Ministry for the Environment, Nature Conservation, Building and Nuclear Safety under contract number 0325491.

References

[1] Benick, J., et al. High-efficiency n-type silicon solar cells with front side boron emitter. in Proceedings of the 24th European Photovoltaic Solar Energy Conference. 2009. Hamburg, Germany.

[2] Cousins, P.J., et al. Generation 3: improved performance at lower cost. in Proceedings of the 35th IEEE Photovoltaic Specialists Conference. 2010. Honolulu, Hawaii USA.

[3] Geerligs, L.J. and D. Macdonald, Base doping and recombination activity of impurities in crystalline silicon solar cells. Progress in Photovoltaics: Research and Applications, 2004. 12(4): p. 309-16.

[4] Romijn, I.G., et al. Optimizing Screen Printed n-type Solar Cells Towards 20% Efficiency. in SolarCon/CPTIC China. 2012. Shanghai, China.

[5] Bueno, G., et al. Simultaneous diffusion of screen printed boron and phosphorus paste for bifacial silicon solar cells. in Proceedings of the 20th European Photovoltaic Solar Energy Conference. 2005. Barcelona, Spain.
[6] B. Bazer-Bachi, C.O., B. Semmache, Y. Pellegrin, M. Gauthier, N. Le Quang, M. Lemiti. CO-DIFFUSION FROM BORON DOPED OXIDE AND POCL3. in Proceedings of the 26th European Photovoltaic Solar Energy Conference and Exhibition. 2011. Hamburg, Germany.
[7] Wehmeier, N., et al. BORON-DOPED PECVD SILICON OXIDES AS DIFFUSION SOURCES FOR SIMPLIFIED HIGH-EFFICIENCY SOLAR CELL FABRICATION. in EUPVSEC 13. 2013. Paris.
[8] Sheoran, M., et al. Ion-implant doped large-area n-type Czochralski high-efficiency industrial solar cells in Photovoltaic Specialists Conference (PVSC). 2012.
[9] Rothhardt, P., et al., Co-diffusion from APCVD BSG and $POCl_3$ for Industrial n-type Solar Cells. Energy Procedia, 2013. 38(0): p. 305-11.
[10] Rothhardt, P., et al. Control of phosphorus doping profiles for co-diffusion processes. in Proceedings of the 27th European Photovoltaic Solar Energy Conference and Exhibition. 2012. Frankfurt, Germany.
[11] Richter, A., et al. Firing stable Al_2O_3/SiNx layer stack passivation for the front side boron emitter of n-type silicon solar cells. in Proceedings of the 25th European Photovoltaic Solar Energy Conference and Exhibition. 2010. Valencia, Spain.
[12] Fellmeth, T., F. Clement, and D. Biro, Analytical Modeling of Industrial-Related Silicon Solar Cells IEEE JOURNAL OF PHOTOVOLTAICS, 2013. PP(99): p. 1-10.
[13] Rothhardt, P., et al., Characterization of POCl3-Based Codiffusion Processes for Bifacial N-Type Solar Cells. IEEE JOURNAL OF PHOTOVOLTAICS, 2014. accepted.
[14] Miyake, M., Diffusion of Boron into Silicon from Borosilicate Glass Using Rapid Thermal Processing. Journal of the Electrochemical Society, 1991. 138(10): p. 3031-3039.